PCCP

Accepted Manuscript

ROYAL SOCIETY OF CHEMISTRY

www.rsc.org/pccp

How many bound valence states does the C_{60}^- anion have?

Evgeniy V. Gromov,*[,†,‡] Shachar Klaiman,[¶] and Lorenz S. Cederbaum[¶]

[†]*Department of Biomolecular Mechanisms, Max-Planck Institute for Medical Research Jahnstraße 29, D-69120 Heidelberg, Germany*

[‡]*Laboratory of Quantum Chemistry, Computer Center, Irkutsk State University K. Marks 1, 664003 Irkutsk, Russian Federation*

[¶]*Theoretische Chemie, Physikalisch-Chemisches Institut, Universität Heidelberg Im Neuenheimer Feld 229, D-69120 Heidelberg, Germany*

*evgeniy.gromov@mpimf-heidelberg.mpg.de

Abstract

We report on unprecedentedly large coupled cluster calculations for the C_{60}^- anion, and on a heuristic model uncovering the valence states of C_{60}^- that allow to resolve the headlined question. Our results convincingly demonstrate that C_{60}^- possesses as many as four bound valence states: $^2T_{1u}$, $^2T_{1g}$, $^2T_{2u}$ and ^2H_g. Our findings reconcile previous controversies regarding the existence of the bound $^2T_{2u}$ and ^2H_g states. For all bound states of C_{60}^- we present an analysis of the radial and angular distribution of the excess electron, which reveals some unique properties of the valence states. Some interesting features of the introduced model are analyzed and discussed.

One of remarkable properties of the Buckminsterfullerene (C_{60}) is its extraordinary electron-accepting ability, which makes C_{60} a peculiar species that is able to form stable mono- (C_{60}^{-}) and poly- (C_{60}^{n-}) anions.[1] It is virtually this property that has determined a large interest in C_{60} in various fields of science and technology. Prominent examples of this interest include prospects of designing with C_{60} new electronic devices, such as molecular transistors, molecular junctions and organic solar cells.[2–5] Closely related to the C_{60}^{-} anion are alkali-doped C_{60} endohedral species, which are considered promising superconducting materials.[6,7] A new strong interest in C_{60}^{-} has emerged recently from the discovery of superatomic like (SAMO) states.[8,9] These states were shown to exhibit remarkable properties, suggesting some new exciting applications of C_{60}.[10]

In this work we focus on the C_{60}^{-} anion, which can be undoubtedly considered a peculiar species. Unlike the majority of molecular anions, which possess only one stable (bound) anion state, C_{60}^{-} exhibits *several* such states, that is there exist several bound C_{60}^{-*} excited states. This peculiarity was proposed to make C_{60} and its derivatives particularly suitable in designing efficient bulk heterojunction that are considered most promising in the construction of organic solar cells.[11] A remarkable aspect related to the C_{60}^{-*} states is that they are all *correlation-bound*, that is these states are unbound at the Hartree-Fock level.[12] A recently obtained interesting finding related to the bound states of C_{60}^{-} is that they are of different type/nature.[12,13] Specifically, there are three *valence* like states, $^2T_{1u}$, $^2T_{1g}$ and $^2T_{2u}$, and one *non-valence*, ^2A_g state correlating with the aforementioned SAMO state.[12,14] Spanning a large range of electron binding energy (EBE), from 2.42 eV for $^2T_{1u}$ to 0.14 eV for $^2T_{2u}$, the valence states were revealed to exhibit nearly identical radial distribution of the excess electron, which differs substantially from that of the ^2A_g SAMO state.[13,15] The distinctive characteristic of the C_{60}^{-} valence states was shown to be the angular distribution of the excess electron, which accounts for the variance of EBEs of these states. Importantly, the electron correlation effects, which play crucial roles in binding the excess electron in the C_{60}^{-} valence states, were found to predominate in the angular distribution rather than in the radial one.[13]

Although many experimental and theoretical efforts in studying C_{60}^{-} have been made, some questions still exist. In particular, the fundamental question of *how many bound electronic states does* C_{60}^{-} *have* still remains open. From the experimental side, most of the previous studies focused mainly on the $^2T_{1u}$ ground state of C_{60}^{-} (see Ref. 16 and references

therein). There are only a few works where excited states of C_{60}^- were addressed.[17–19] In this way, only the lowest excited state ($^2T_{1g}$) was clearly observed. At the same time, previous theoretical investigations predicted several bound excited states of C_{60}^-.[12,14,18,20] There are, however strong contradictions and deviations among the theoretical results, in particular concerning the ^2H_g, $^2T_{2u}$ and ^2A_g excited states.[12,20,21]

In a recent work,[12] we made a considerable step forward towards answering the above question, having identified four bound states of C_{60}^-, $^2T_{1u}$, $^2T_{1g}$, $^2T_{2u}$ and ^2A_g, mentioned above. In the present work we aim at unveiling *all bound valence* states of C_{60}^-, thereby almost completely resolving this question. Our approach rests on results of high-level ab initio coupled cluster (CC) calculations and predictions of a heuristic model. In the following, we first present the results of our CC calculations, which uncover a new bound state, in addition to the four previously found states. We will characterize this new state against the other states using a density analysis.[13] Finally, we will present the results of the heuristic model, which fully support our CC findings and allow to answer the question about the complete set of the valence bound states of C_{60}^-.

In order to reveal all the bound valence states of C_{60}^- we performed unprecedentedly large CC calculations.[22] In these calculations, the state-of-the-art EA-EOM-CCSD method[23] was used in combination with a basis set of the triple-ζ quality. More specifically, we employed at each carbon atom the triple-ζ basis set of Dunning (cc-pVTZ),[24] without the *f*-type functions, augmented with one *s*-type diffuse function from the corresponding aug-cc-pVTZ basis set.[24] This was further augmented with a set of $6s$, $6p$ and $6d$ diffuse functions placed in the center of C_{60}.[25] In the following we refer to this basis as TZ(+s)(-f)+6s6p6d. The total number of molecular orbitals (MOs) in our CC calculations with this basis set amounted to 1494. To the best of our knowledge these are the largest and most accurate calculations for the C_{60}^- anion to date. For the purpose of analysis we also carried out calculations using a smaller basis set. In all the calculations, we used the geometry of the neutral C_{60} molecule, with C–C bond lengths of 1.458 Å and 1.401 Å, taken from an electron diffraction experiment.[26] In all CC calculations, the D_{2h} point group, a subgroup of the full (I_h) point group of C_{60}, was utilized. All CC computations were performed with the CFOUR package.[27]

The results of our EA-EOM-CCSD calculations are presented in Figure 1. Our major finding here is the prediction of a new bound state, ^2H_g, with EBE of 56 meV. This result improves on our previous findings, obtained with a basis set of the double-ζ quality (Fig.

1, the DZ(+s)+6s6p6d data set), where this state was predicted unbound.[12] According to the present results, the C_{60}^- anion has overall five bound anion states, ^2H_g, ^2A_g, $^2T_{2u}$ $^2T_{1g}$ and $^2T_{1u}$ in order of increasing EBEs. Note that the $^2T_{1u}$, $^2T_{1g}$, $^2T_{2u}$ and ^2H_g states are degenerate at the geometry of the neutral C_{60}, with $^2T_{1u}$, $^2T_{1g}$ and $^2T_{2u}$ being composed of three components each, while ^2H_g has five components. If one considers the Jahn-Teller distortion of the C_{60}^- anion, then some of these degeneracies are lifted and the total number of states will be larger than at the geometry of the neutral C_{60}. We will not address this point further in the present work.

Interestingly, a ^2H_g state was invoked in an early experimental study[28] to account for a visible absorption band of C_{60}^- in solution. In a previous theoretical work,[20] the ^2H_g state was found to be bound, but its EBE was largely overestimated. At the same time, in a recent theoretical study,[21] this state was predicted to be largely unbound. Looking ahead, the found ^2H_g state is a valence-type state. It should therefore exhibit the same intrinsic properties as the other valence states of C_{60}^-.

Clearly, the observed binding of the ^2H_g state results from improving the basis set on the carbon atoms, from DZ(+s) to TZ(+s)(-f). To shed some more light on the origin of the binding we performed calculations with an extended DZ(+s) basis set at the carbon atoms, which contained two sets of polarization *d*-functions taken from the cc-pVTZ basis (no diffuse central functions were included). As can be seen (Fig. 1, the DZ(+s)(2d) results), the ^2H_g state is predicted to be bound when employing the latter basis set. This result suggests that polarization effects in the C_{60} neutral and anion states, which are obviously better described by the two sets of *d*-functions, make an important contribution to the binding of this state. One can thus consider ^2H_g to be another polarization bound state of the C_{60}^- anion, along with the $^2T_{2u}$ state.[12]

From comparison of the TZ(+s)(-f)+6s6p6d and DZ(+s)+6s6p6d results, there is a notable increase (stabilization) in EBEs of the other valence states, $^2T_{1u}$, $^2T_{1g}$ and $^2T_{2u}$, upon switching to the TZ(+s)(-f) basis set at the carbon frame. This is an expected "reaction" of the valence states to improving the description of the valence shells of the carbon atoms. By contrast, the ^2A_g SAMO state undergoes very little stabilization, which relates to its different, non-valence character. Noteworthy, among the valence states, $^2T_{2u}$ and ^2H_g are seen to experience the largest stabilization, which amounts to ∼100 meV and ∼90 meV, respectively. This confirms the above mentioned similarity between the two states, related

to their polarization bound character.

Note that our present best predictions of EBEs for the four valence states still might be somewhat underestimated because of the lack of higher angular momentum basis functions in the TZ(+s)(-f)+6s6p6d basis set. This follows from the fact that the $^2T_{1u}$ and $^2T_{2u}$, and $^2T_{1g}$ and ^2H_g states transform as the L=5 and L=6 spherical harmonics, respectively.[29] The presence of the *f*- and *g*-type functions should therefore very likely lead to a further stabilization of these states. In accordance with the latter, we found the stabilization due to the *f*-functions to be ∼100 meV for the valence states of a smaller fullerene.[30] Elucidating the effect of the *f*-functions on the EBEs of the C_{60}^- states is at present not possible due to the prohibitively large size (∼1900 MOs) of the EA-EOM-CCSD calculations.

From the above discussion, the EBEs of all the states under considerations should be expected to increase with further enlarging (improving) the basis set. One can also expect increasing the EBEs of at least all excited bound states of C_{60}^- if one further improves the method, with respect to description of the electron correlation, by accounting for higher (triple, quadruple, etc) electron excitations. The latter follows from the fact that all the excited bound states of C_{60}^- are correlation bound. This strongly suggests that additional electron correlation, which might be missing at the current (EA-EOM-CCSD) level of theory, will only lead to further binding of these states. Accordingly, the predicted bound states of C_{60}^- are expected to remain bound even at the full configuration interaction (FCI) and complete basis set (CBS) limit.

Besides the EBEs, we have also computed for each anion state under consideration a natural orbital expansion of reduced density. This allowed us to analyze the electronic structure of the states, in particular, as far as the distribution of the excess electron is concerned. In the following, we present the results of the so-called $\Delta\rho$ analysis.[13] The latter is based on analysis of the difference of the anion's $\rho_{\mathrm{A}}(\mathbf{r})$ and neutral's $\rho_{\mathrm{N}}(\mathbf{r})$ charge densities:

$$\Delta\rho(\mathbf{r}) = \rho_{\mathrm{A}}(\mathbf{r}) - \rho_{\mathrm{N}}(\mathbf{r})$$

where $\mathbf{r}$ denotes in general a set of nuclear and electronic coordinates. The quantity $\Delta\rho(\mathbf{r})$ reflects changing of the total charge density upon "transition" from the neutral to the anion species. It can be both positive and negative. Positive values of $\Delta\rho(\mathbf{r})$ are indicative of the excess negative charge, associated with the excess electron density, while negative $\Delta\rho(\mathbf{r})$ points out to a decrease of the neutral's electron density in the anion state. By casting

$\Delta\rho(\mathbf{r})$ into the form of radial, $\Delta\rho(r)$, and angular, $\Delta\rho(\varphi,\theta)$, distributions (for the definition of r, φ and θ spherical coordinates see electronic supplementary information of Ref. 13) one obtains useful information on the distribution of the excess electron, which can be easily analyzed.

The calculated radial (RD) and angular (AD) distributions of the excess electron in the five anion states of C_{60}^- are shown in Figures 2 and 3, respectively. Here, we focus mainly on the newly found bound ^2H_g state. For the other states, the present RD and AD reproduce those calculated with the DZ(+s)+6s6p6d basis set, presented and discussed in Ref. 13. They are shown here to facilitate the discussion for the ^2H_g state. As can be seen, the RD of the ^2H_g state is very similar to the distribution of the other valence states and clearly differs from that of the ^2A_g SAMO state (Fig. 2). This unambiguously points out to the valence like character of the ^2H_g state. Noteworthy, the RD of the ^2H_g state turns out to be more close to that of the $^2T_{2u}$ state than to the RDs of the two other valence states. This can be seen well from the total excess charge shown in the inset of Fig. 2. This is further evidence of the similarity between the ^2H_g and $^2T_{2u}$ polarization states. As expected, the difference between the ^2H_g and other valence states lies in the angular distribution of the excess electron, which can be clearly seen in Fig. 3. The most delocalized pattern of AD in the case of the ^2H_g state, as compared with the other valence states, accounts for its smallest EBE value.

Our high-level electronic structure calculations presented above have allowed for unraveling the four bound valence states of C_{60}^-. In the following we aim to show that this set of states is complete, that is no other bound valence states should be expected. To this end we introduce a simple, yet efficient *heuristic* model. It comprises a neutral C_{60} with a positive point charge in its center (in the following denoted C_{60}(+q)). Let us consider "anion" states, i.e. with an extra electron, of C_{60}(+q). Obviously, the presence of the positive charge will lead to stabilization of all such states. Depending on the magnitude of the charge, some states will become bound already at the level of Koopman's theorem. It is interesting to find out which states get thus bound, in particular which are the *lowest* bound anion states of C_{60}(+q) for a given charge q. To answer this, we will smoothly vary the magnitude of the charge, from 0.0 to +2.0, to trace the formation of the "anionic" bound states. We emphasize that we are interested in the lowest unoccupied MOs of C_{60}(+q), which are obtained from nothing but the corresponding Hartree-Fock calculation.

The results for the C_{60}(+q) model are presented in Figure 4, panels *a* and *b*. In the panels are shown the energies of several lowest unoccupied MOs (which are EAs according to Koopman's theorem) as functions of the point charge value. The results in panel *a* were obtained with the cc-pVDZ basis set, while those in panel *b* were calculated using the cc-pVQZ one. All calculations were performed within the I_h point group, employing the Turbomole package.[31] We first discuss the results obtained with the cc-pVDZ basis (Fig 4a). The latter basis can be considered sort of a "minimal" basis set for C_{60}, at which only the *valence* orbitals should be expected among the lowest unoccupied MOs. Accordingly, the MOs presented in Fig. 4a are associated with the valence anion states of C_{60}^-. An important observation to be inferred from Fig. 4a is that one can distinguish among these states the following two groups of states: $7t_{1u}$, $3t_{1g}$, $7t_{2u}$ and $11h_g$ – the first group, and $7h_u$ and $7g_g$ – the second one. Clearly, the first group of states explicitly correlates with the four bound valence states of C_{60}^- considered above. The model predicts these states to be all bound (have negative ϵ) at q$\sim$0.8 a.u. As can be seen, the order of the bound states is consistent with that obtained from the EA-EOM-CCSD calculations. One can also note that the model predicts a small energy gap between the ^2H_g and $^2T_{2u}$ states ($\sim$0.1 eV), and a much larger gap between $^2T_{2u}$ and $^2T_{1g}$ ($\sim$1 eV), and $^2T_{1g}$ and $^2T_{1u}$ ($\sim$1.5 eV), which is in *qualitative* agreement with the EA-EOM-CCSD results. Let us now look at the situation at q$\sim$1.6 a.u. At this charge the next valence state, ^2H_u, becomes also bound. Importantly, the gap between the latter state and the ^2H_g state is very large, $\sim$2.5 eV. Tracing this result back to the C_{60}^- anion, one should expect the ^2H_u state at least 1 or 2 eV higher in energy than the ^2H_g state. The latter obviously suggests ^2H_u to be (largely) unbound. The ^2H_g state is thus the last bound valence state of C_{60}^-.

The results in Fig 4a might be argued to need verification with regard to their convergence with respect to the basis set. Such a verification is provided in Fig. 4b. As can be inferred, the above two groups of states fully persist at the cc-pVQZ basis set. At the same time, one sees that besides these two groups there is a third one, which comprises two states associated with the excess electron in orbital $5a_g$ and $8t_{1u}$. These two states are seen to exhibit completely different dependence on the charge than the valence states, in particular being much stronger stabilized as the charge increases. The latter behavior can be shown to be characteristic of the SAMO states. Indeed, as can be seen from Fig. 2 (see also the discussion in Refs. 13,15), the ^2A_g SAMO state exhibits some excess electron density inside

the C_{60} hollow. Therefore, it is to be expected to experience a much stronger stabilization by the central charge than the valence states, which do not show such a feature. The same holds for the second, $8t_{1u}$ state, which is a *p*-type SAMO state. This state was recently addressed in the work of Ref. 32, where based on model potential calculations it was predicted to be unbound. Our present EA-EOM-CCSD calculations also predict this state unbound by 61 meV. Note that the appearance of the SAMO states in Fig. 4b relates to the use of cc-pVQZ basis set. The large size of this basis (3300 MOs for C_{60}) apparently allows for a partial description of the SAMO states, in particular their parts inside the C_{60} hollow.

From the above discussion, the predictions of the C_{60}(+q) model for the valence states of C_{60}^-, obtained with the double-ζ and quadruple-ζ basis sets, are entirely consistent. Moreover, they fully persist upon further expansion of the basis to cc-pV5Z (5460 MOs). Thus we can confidently conclude that C_{60}^- possesses as many as four bound valence states, $^2T_{1u}$, $^2T_{1g}$, $^2T_{2u}$ and ^2H_g. Remarkably, in the case of the quadruple-ζ basis set the C_{60}(+q) model correctly predicts possible SAMO states of C_{60}^-. These states can be readily distinguished from the valence states based on their much stronger stabilization due to the central charge, resulting in the steeper curves in comparison with those obtained for the valence states (Fig. 4b). Noteworthy, all the valence states are characterized by almost the same slope of the curves, i.e., the curves are parallel. Furthermore, the valence curves fit very well to linear regressions, with the states within the same group exhibiting close fitting parameters. This trend is a consequence of the fact that all the valence states are characterized by similar RDs of the excess electron. Importantly, the charge in the center of C_{60} entails little alteration of the RDs, resulting merely in lowering the energy of the states. This lowering is due to nothing but Coulomb attraction between the central charge and the excess electron. Indeed, for the $^2T_{1u}$ state, one obtains the Coulomb attraction (energy lowering) of $\sim$3.14 eV in the case of charge being 1.0 a.u. This gives the distance between the positive charge and the excess electron to be 8.67 bohr. The latter value is in excellent agreement with the maximum of the RD for the $^2T_{1u}$ state (Fig. 2). Clearly, the same holds for the other bound valence states of C_{60}^-, which exhibit the same slope of the lines (Fig. 4a,b) and the same RD maximum as the $^2T_{1u}$ state (Fig. 2).

At the end, we briefly discuss the question of experimental observation of the bound excited states of C_{60}^-. As has been mentioned in the beginning, there is so far only a clear observation of the $^2T_{1g}$ state, in particular in the pump-probe experiment by Ehrler

and co-workers.[18] In this experiment, transitions from the $^2T_{1u}$ ground state to the $^2T_{1g}$ first excited state of C_{60}^- were stimulated by a pump pulse, followed by their detection by measuring corresponding photoelectrons pulled off by a probe pulse. We suggest that a similar experiment can be performed to observe the bound ^2H_g state. The reason is, the probability of the $^2T_{1u}\rightarrow{}^2H_g$ transition is expected to be comparable to that of the $^2T_{1u}\rightarrow{}^2T_{1g}$. This in turn follows from that the corresponding transition dipole moments should be similar, because both the $^2T_{1g}$ and ^2H_g states are of the same valence type, which was shown to lead to similar properties of the states. The same would hold for the $^2T_{2u}$ state, but the $^2T_{1u}\rightarrow{}^2T_{2u}$ transition is dipole forbidden. By contrast, the ^2A_g SAMO state differs substantially from the valence states and one should expect the transition dipole moment for $^2T_{1u}\rightarrow{}^2A_g$ to be small due to the very diffuse character of the ^2A_g state. Our preliminary EA-EOM-CCSD calculations for the oscillator strengths of the mentioned transitions fully confirm our reasoning.

In conclusion, using the state-of-the-art EA-EOM-CCSD method and the triple-ζ quality basis set we have performed large-scale calculations that unraveled five bound states of C_{60}^-. These are four valence like states, ^2H_g, $^2T_{2u}$, $^2T_{1g}$ and $^2T_{1u}$ and one superatomic like (SAMO) ^2A_g state. Whereas the three valence states, $^2T_{2u}$, $^2T_{1g}$ and $^2T_{1u}$, and the SAMO state have already been known,[12] the existence of the bound ^2H_g state remained open and has been fully resolved only here. From the present results, ^2H_g turns out to be another polarization bound state of C_{60}^-, in addition to the $^2T_{2u}$ state. Like all the other valence states, ^2H_g exhibits the same radial distribution and different angular distribution of the excess electron in comparison with the other valence states. Noteworthy, having the lowest binding energy of ~ 56 meV, ^2H_g turns out to be the last bound valence state of C_{60}^-. The latter has been revealed based on the heuristic C_{60}(+q) charge model. This model works perfectly in the case of C_{60}, where the group of the bound and unbound valence states can be discerned. Besides the valence states, the model correctly predicts possible superatomic like states of C_{60}^-, namely, the *s*-type ^2A_g and the *p*-type $^2T_{1u}$ SAMO states. Given that the *p*-type state has been predicted unbound, by the present large-scale ab initio as well as previous model[32] computations, we come to the conclusion that the above five states constitute the *complete* spectrum of the bound states of C_{60}^-.

We would like to emphasize that our work resolves contradictions that emerged from the study of Ref. 21. Our present results are fully consistent with our previous findings, Ref. 12,

as far as the $^2T_{1u}$, $^2T_{1g}$, $^2T_{2u}$ and ^2A_g states are concerned. For the $^2T_{1u}$ and $^2T_{1g}$ states, the obtained EBEs agree fairly well with the available experimental data. The existence of the bound ^2H_g state clearly follows from the heuristic C_{60}(+q) model and has been confirmed by our coupled-cluster calculations. The fact that the authors of Ref. 21 found only two out of five bound anion states points out to very special or/and strong correlation effects in these states, which seemingly cannot be reliably described by the methods based on perturbation theory, at least when a low (second or third) order perturbation treatment is invoked (see also the discussion in Ref. 12). Finally, in this work we introduced a simple heuristic model to predict possible bound valence states and possible SAMO states of the C_{60}^- anion. The model has shown its efficacy, which suggests its possible application to other caged fullerenes. It is thus worthwhile to further address this model and to attempt its developing as far as possible. In this context, application of this model to large fullerenes, for which high-level ab initio calculations are yet not possible, would be an exciting perspective.

ACKNOWLEDGEMENTS

Financial support of the Deutsche Forschungsgemeinschaft (DFG) is gratefully acknowledged. This research was supported in part by the bwHPC initiative and the bwHPC-C5 project (bwHPC and bwHPC-C5 (http://www.bwhpc-c5.de) funded by the Ministry of Science, Research and the Arts Baden-Württemberg (MWK) and the Germany Research Foundation (DFG)) provided through associated compute services of the JUSTUS HPC facility at the University of Ulm. We wish to thank the support/system-administration team of JUSTUS for providing us with the extended queue for our demanding computations. We also thank the high performance computer center Helics3a (Heidelberger Linux Cluster System, http://helics.uni-hd.de) for the computational resources. E.V.G. wishes to thank Uwe Huniar for the support with the use of the Turbomole package.

[1] C. A. Reed and R. D. Bolskar, Chem. Rev. **100**, 1075 (2000).

[2] M. Prato, J. Mater. Chem. **7**, 1097 (1997).

[3] H. Park, J. Park, A. K. L. Lim, E. H. Anderson, A. P. Alivisatos, and P. L. McEuen, Nature (London) **407**, 57 (2000).

[4] X.-J. Zhang, M.-Q. Long, K.-Q. Chen, Z. Shuai, Q. Wan, B. S. Zou, and Z. Zhang, Appl. Phys. Lett. **94**, 073503 (2009).

[5] J. L. Segura, N. Martin, and D. M. Guldi, Chem. Soc. Rev. **34**, 3147 (2005).

[6] R. C. Haddon, A. F. Hebard, M. J. Rosseinsky, D. W. Murphy, S. J. Duclos, K. B. Lyons, B. Miller, J. M. Rosamilia, R. M. Fleming, A. R. Kortan, S. H. Glarum, A. V. Makhija, A. J. Muller, R. H. Eick, S. M. Zahurak, R. Tycko, G. Dabbagh, and F. A. Thiel, Nature **350**, 320 (1991).

[7] A. F. Hebard, R. C. Haddon, D. W. Murphy, S. H. Glarum, T. T. M. Palstra, A. P. Ramirez, and A. R. Kortan, Nature **350**, 600 (1991).

[8] M. Feng, J. Zhao, and H. Petek, Science **320**, 359 (2008).

[9] M. Feng, J. Zhao, T. Huang, X. Zhu, and H. Petek, Acc. Chem. Res. **44**, 360 (2011).

[10] J. Zhao, M. Feng, J. Yang, and H. Petek, Nano **3**, 853 (2009).

[11] T. Liu and A. Troisi, Adv. Mater. **25**, 1038 (2013).

[12] S. Klaiman, E. V. Gromov, and L. S. Cederbaum, J. Phys. Chem. Lett. **4**, 3319 (2013).

[13] S. Klaiman, E. V. Gromov, and L. S. Cederbaum, Phys. Chem. Chem. Phys. **16**, 13287 (2014).

[14] V. K. Voora, K. D. Jordan, and L. S. Cederbaum, J. Phys. Chem. Lett. **4**, 849 (2013).

[15] E. V. Gromov, S. Klaiman, and L. S. Cederbaum, Mol. Phys. **113**, 2964 (2015).

[16] D.-L. Huang, P. D. Dau, H.-T. Liu, and L.-S. Wang, J. Chem. Phys. **140**, 224315 (2014).

[17] S. Tomita, J. U. Andersen, E. Bonderup, P. Hvelplund, B. Lui, S. B. Nielsen, U. V. Pedersen, J. Rangama, K. Hansen, and O. Echt, Phys. Rev. Lett. **94**, 53002 (2005).

[18] O. T. Ehler, J. P. Yang, C. Hättig, A.-N. Unterreiner, H. Hippler, and M. M. Kappes, J. Chem. Phys. **125**, 074312 (2006).

[19] K. Støchkel and J. U. Andersen, J. Chem. Phys. **139**, 164304 (2013).

[20] V. P. Vysotskiy and L. S. Cederbaum, J. Chem. Phys. **132**, 044110 (2010).

[21] V. G. Zakrzewski, O. Dolgounitcheva, and J. V. Ortiz, J. Phys. Chem. A **118**, 7424 (2014).

[22] The most demanding part of the coupled cluster calculations required more than 128 GB of RAM-memory, about 10 TB of disk space and about 4 weeks of computation time at the high-performance compute resource JUSTUS (University of Ulm). The average computation time for each anion state amounted to one month.

[23] M. Nooijen and R. J. Bartlett, J. Chem. Phys. **102**, 3629 (1995).

[24] T.H. Dunning, Jr., J. Chem. Phys. **90**, 1007 (1989).

[25] The exponents of the $6s$, $6p$ and $6d$ diffuse functions in the center of C_{60} were generated using an even-tempered series $\alpha_{n+1} = \alpha_n/3.5$, starting with $\alpha_0 = 1.0$.

[26] K. Hedberg, L. Hedberg, D. S. Bethune, C. A. Brown, H. C. Dorn, R. D. Johnson, and M. D. Vries, Science **254**, 410 (1991).

[27] CFOUR, Coupled-Cluster techniques for Computational Chemistry, a quantum-chemical program package by J. F. Stanton, J. Gauss, M. E. Harding, P. G. Szalay, with contributions from A. A. Auer, R. J. Bartlett, U. Benedikt, C. Berger, D. E. Bernholdt, Y. J. Bomble, L. Cheng, O. Christiansen, M. Heckert, O. Heun, C. Huber, T.-C. Jagau, D. Jonsson, J. Jusélius, K. Klein, W. J. Lauderdale, D. A. Matthews, T. Metzroth, L. A. Mück, D. P. O'Neill, D. R. Price, E. Prochnow, C. Puzzarini, K. Ruud, F. Schiffmann, W. Schwalbach, C. Simmons, S. Stopkowicz, A. Tajti, J. Vázquez, F. Wang, J. D. Watts and the integral packages MOLECULE (J. Almlöf and P. R. Taylor), PROPS (P. R. Taylor), ABACUS (T. Helgaker, H. J. Aa. Jensen, P. Jørgensen, and J. Olsen), and ECP routines by A. V. Mitin and C. van Wüllen. For the current version, see http://www.cfour.de.

[28] T. Kato, Laser Chem. **14**, 155 (1994).

[29] F. Rioux, J. Chem. Educ. **71**, 464 (1994).

[30] E. V. Gromov, S. Klaiman, and L. S. Cederbaum, Bound anion states of C_{36}^- (unpublished).

[31] R. Ahlrichs, M. Bär, M. Häser, H. Horn, and C. Kölmel, Chem. Phys. Lett. **162**, 165 (1989).

[32] V. K. Voora and K. D. Jordan, Nano Lett. **14**, 4602 (2014).

[33] J. C. Rienstra-Kiracofe, G. S. Tschumper, H. F. S. III, S. Nandi, and G. B. Ellison, Chem. Rev. **102**, 231 (2002).

FIGURE CAPTIONS

Figure 1. The energies of the C_{60}^- states (EBEs for the bound states) calculated using the EA-EOM-CCSD method and different basis sets, and the experimental electron affinities (Exp) taken from Ref. 16,18. The experimental data are adiabaitic values, i.e., the difference between the neutral's energy at the neutral's geometry and the anion's energy at the anion's geometry.[33] These are by definition larger than *vertical* EBEs calculated here, i.e., the energy difference at the neutral's geometry. The origin (dashed line) corresponds to the ground state of the neutral C_{60}. The DZ(+s)+6s6p6d results are taken from the work of Ref. 12. The ^2H_g and $^2T_{2u}$ are polarization-bound states and are emphasized in red and blue, respectively.

Figure 2. Radial distributions of the excess electron density ($\Delta\rho(r)$) for the four bound valences states, $^2T_{1u}$, $^2T_{1g}$, $^2T_{2u}$, ^2H_g, and a bound ^2A_g SAMO state of the C_{60}^- anion. The dashed horizontal line stands for the radius of C_{60}. Note that all valence states exhibit similar radial distributions. The inset shows the total excess charge q_{excess} (disregarding the sign) for each state, calculated by integrating the corresponding $\Delta\rho(r)$ over r from zero to r. The value of q_{excess} at a particular r is the total excess charge encompassed with a sphere of radius r.

Figure 3. Angular distribution of the excess electron density for the four valence states of C_{60}^-, $^2T_{1u}$ (a), $^2T_{1g}$ (b), $^2T_{2u}$ (c) and ^2H_g (d). The range of both the azimuthal (θ) and polar (φ) angles is from 0 to π. The corresponding distribution for $\pi \leq \theta \leq 2\pi$ is identical since the density is symmetric with respect to θ.

Figure 4. Electron affinities (ε) at the level of Koopman's theorem for the C_{60}(+q) model as functions of the positive charge q at the center of C_{60}: (a) results obtained using the cc-pVDZ basis set; (b) results obtained using the cc-pVQZ basis set. The full lines correspond to the valence states, the dashed lines correspond to the SAMO states.

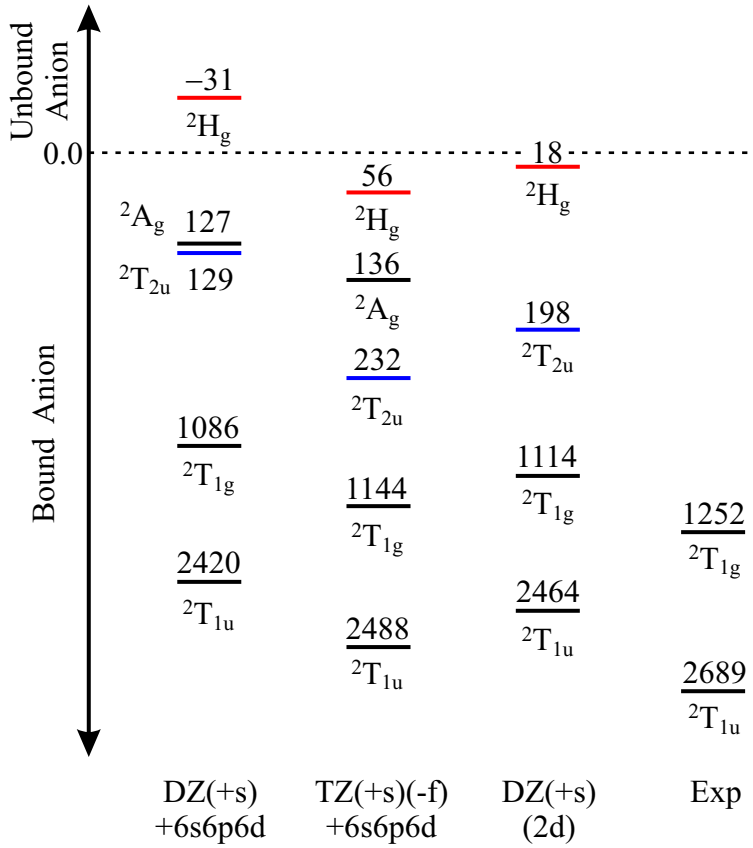

Figure 1.

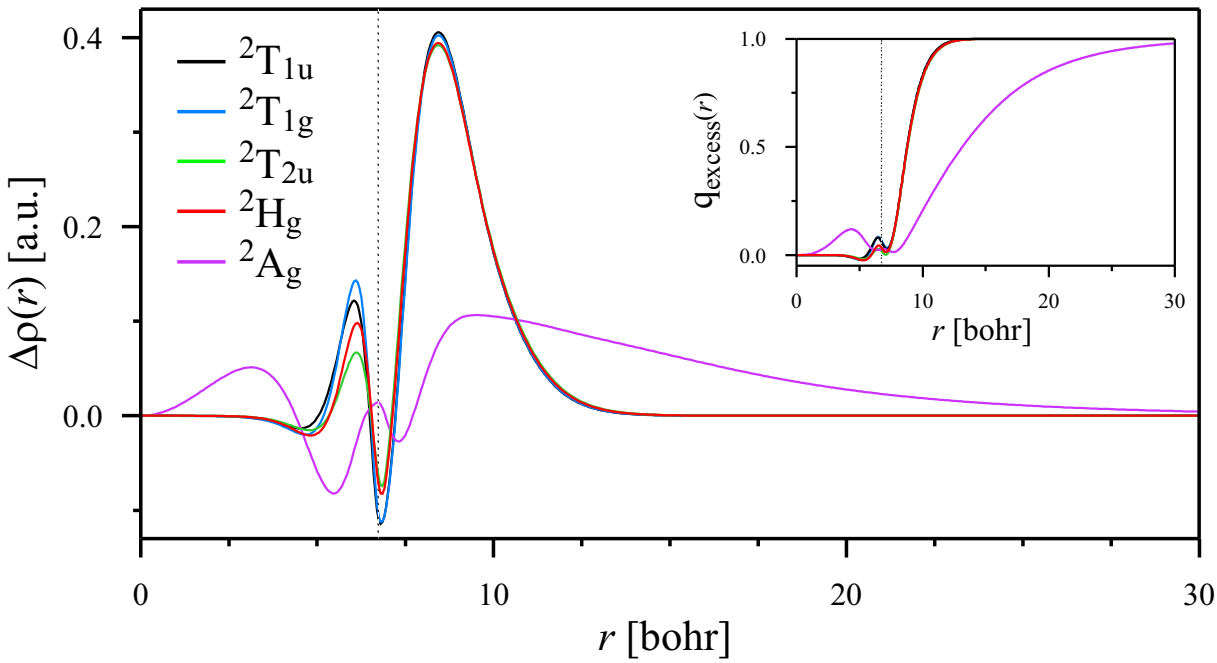

Figure 2.

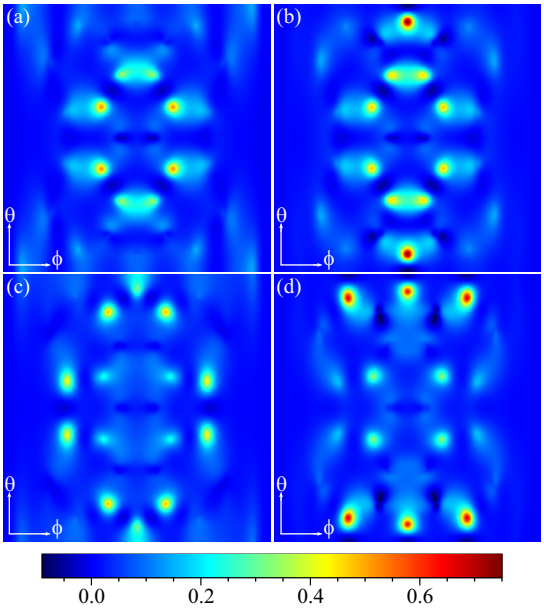

Figure 3.

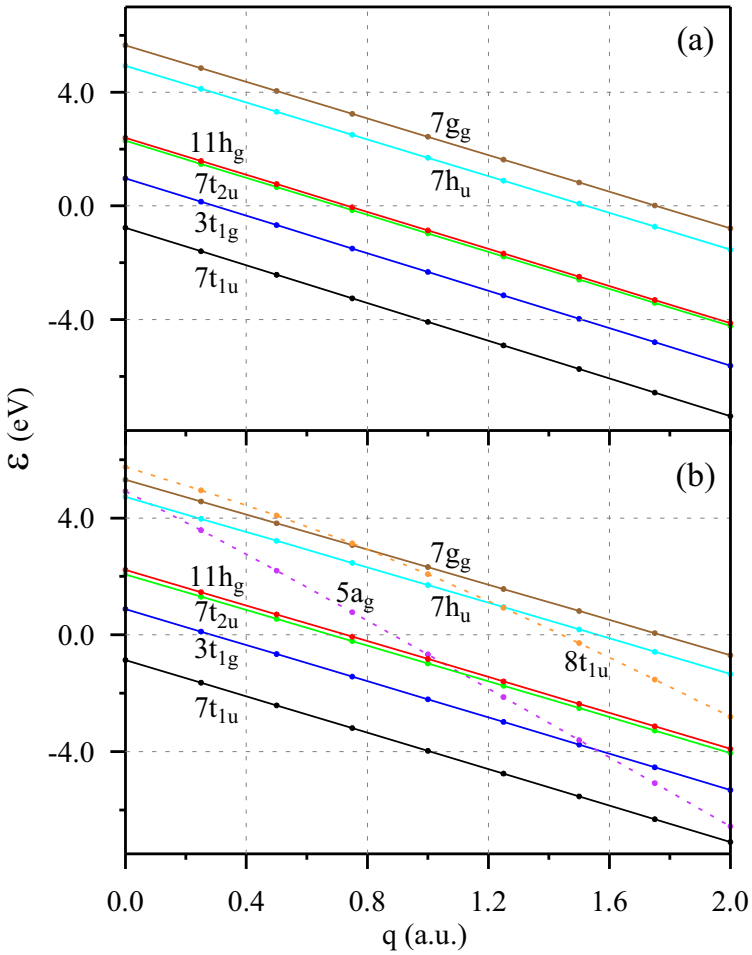

Figure 4.